

# Comparative Study on the Properties of Natural Rubber Composites Containing Kaolin and Calcined Kaolin and on the Possibilities to Apply Thereof as Antenna Substrates

Abdullah G. Al-Sehemi<sup>1,2</sup>, Ahmed A. Al-Ghamdi<sup>3</sup>, Nikolay T. Dishovsky<sup>4\*</sup>, P. Malinova<sup>4</sup>, Nikolay T. Atanasov<sup>5</sup>, Gabriela L. Atanasova<sup>5</sup>

<sup>1</sup>Research Center for Advanced Materials Science (RCAMS), King Khalid University, Abha 61413, P.O. Box 9004, Saudi Arabia.

<sup>2</sup>Department of Chemistry, College of Science, King Khalid University, Abha61413, P.O. Box 9004, Saudi Arabia,

<sup>3</sup>Department of Physics, Faculty of Science, King Abdulaziz University, Jeddah, Saudi Arabia,

<sup>4</sup>Department of Polymer Engineering, University of Chemical Technology and Metallurgy, 1756 Sofia, Bulgaria,

<sup>5</sup>Department of Communication and Computer Engineering, Faculty of Engineering, South-West University 'NeofitRilski', 2400 Blagoevgrad, Bulgaria,

## Abstract

*The idea of combining the advantages of ceramic and polymer materials is not new. But it has become more and more important in recent years because of the improvement of various electronic devices that, in addition to improved parameters, have good mechanical resistance and flexibility.*

*The aim of our study is to obtain composites based on natural rubber(NR) and fillers - standard and three types of calcined kaolin with different particle sizes and in-depth study of their vulcanization characteristics, physico-mechanical, electrical and dielectric properties.*

*A promising application of the developed composites is in the field of wireless communications. For this purpose, a flexible multilayer antenna was prepared in which the composite NR-CK1.3, exhibiting the best dielectric properties, was used as the substrate and insulating layers.*

*The antenna shows much better matching in the frequency ranges of 2.4-2.7 GHz and 5.1-5.4 GHz, compared to cases where the substrates are based on unfilled nitrile butadiene rubber.*

**Keywords** - Kaolin and Calcined Kaolin, Natural Rubber Composites, Physico-mechanical properties, Electrical and dielectric properties

## I. INTRODUCTION

Mechanically flexible or even stretchable electronic systems offering lucrative applications have been gaining great scientific interest [1]. Currently more electronic systems are being worn near or even inside the body. Therefore they must meet a number of requirements concerning their weight, changing of

shape, following all complex movements of particular objects [2]. There are also diverse requirements that an ideal substrate should meet, e.g. low relative permittivity to reduce signal propagation delay, low loss tangent to reduce signal attenuation along with better signal performance, mechanical flexibility, high dimensional stability, moisture absorption resistance, high thermal conductivity to dissipate the heat generated [3-6]. Exhibiting excellent microwave dielectric properties silicates and aluminates turned to be quite suitable for substrate applications amongst low permittivity ceramics [7-9]. In [10] Button et al. report on combining the advantages of ceramic and those of a polymer that has yielded a very satisfactory balance of tailored properties. Besides, the filler used should have permittivity much higher than that of the rubber matrix when aiming preparation of flexible composites with low loss high relative permittivity. Therefore we suggest that kaolin and calcinated kaolin might be appropriate fillers for the purpose.

Kaolin is the most inherent mineral filler used in rubber industry. It accounts for about 54% of the consumption of this type of filler [11]. Its annual consumption in rubber industry is in the range of 172-275 million tonnes [12]. There are basically three reasons: low price (the price ratio of kaolin to that of N330 carbon black within the last twenty years varies in the range of 0.06-0.1), the low consumption of energy for its production - 14 MJ/kg (for comparison the energy consumption for the production of 1 kg of carbon black is 140 MJ/kg) and the relatively good physical and mechanical characteristics of the vulcanizates containing it [13].

Kaolin is identified as a clay mineral kaolinite ( $\text{Al}_2\text{O}_3 \cdot 2\text{SiO}_2 \cdot 2\text{H}_2\text{O}$ ), i.e.  $\text{Al}_2\text{O}_3$ ,  $\text{SiO}_2$  and water are constant components of its composition. It belongs to

the group of so-called layered silicates. There is an ion grid at the base of which there are two structural units in the form of planar nets: silicon-oxygen tetrahedra and alumin-oxygen-hydroxyl octahedrons [14]. Tetrahedra bind in such a way as to form a hexagonal endless repeating mesh that forms a layer of  $[(Si_2O_5)^{2-}]$ . Schematic presentation of the hexagonal network of  $(SiO_4)_4^+$ -tetrahedra is shown in Figure 1.

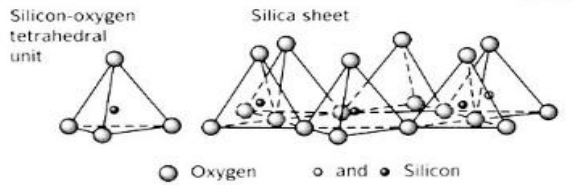


Fig.1. Schematic presentation of  $[SiO_4]$  tetrahedron and a hexagonal network of tetrahedra

The second unit consists of two layers of tightly spaced oxygen atoms and OH-groups, in which octahedral coordination places aluminum atoms so they are equally spaced from six oxygen atoms or OH-groups that occupy the octahedron peaks. In the octahedral network, the octahedrons have common ribs (Fig. 2).

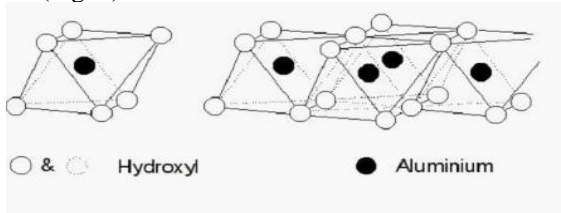


Fig. 2. Schematic presentation of the alumin-octahedron and octahedral network

The silicate packets of kaolin are two-layer and consist of a tetrahedral and octahedral network. The tetrahedrons are  $Si^{4+}$ , and octahedrons -  $Al^{3+}$ , that is why kaolin is di-octadecylic. The crystalline structure of kaolinite is shown in Fig. 3.

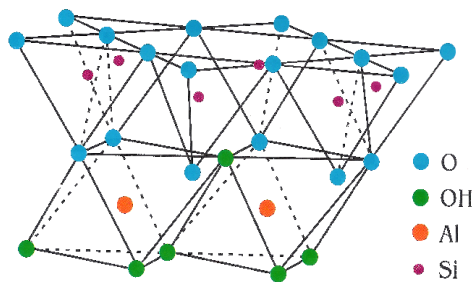


Fig. 3. Crystalline structure of kaolinite

As seen from Fig. 3, the charges in the ideal kaolinite grid are balanced and it is electroneutral. The strong bond between the layers with heterogeneous surfaces of oxygen atoms and OH- groups is achieved due to the hydrogen bond between them. Several possibilities for chemical modification of kaolin have

been described [11,13,15] on the basis that the hydroxyl groups present on the surface of the kaolin particles enter easily and readily into chemical reactions with bifunctional silanes or other modifying agents. An alternative solution to the chemical modification is the thermochemical (sometimes called calcination), in which the chemical composition, volume and surface structure of the kaolin particles can be changed relatively simply and easily under the effect of temperature, and hence all their properties, including those related to their application as fillers in the rubber industry. After separation of the OH- groups, heating results in a significant weakening of the bond strength between the layers, leading to breakage of the crystal lattice and very serious changes in the structure associated with partial amorphousation of the material, as well as the tendency of the parent particles to break into smaller size ones and enhancement of the "filler-filler" interaction, leading to the conformation into secondary structures [16]-Fig.4.

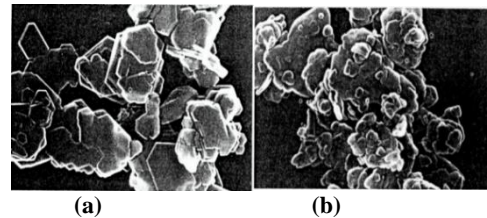


Fig. 4. Electron microscopic photos of standard (a) and calcined (b) kaolin

Given the significant changes in the kaolin structure as described above in its calcination, the aim of the present study is to compare the influence of standard kaolin and three types of calcined kaolin of different particle size on the vulcanization, physico-mechanical, electrical and dielectric properties of composites based on natural rubber. Regarding the electrical properties: influence of chemical nature, structure and particle size of the filler on the specific volume resistance of the composites has been investigated, and the effect of applied external pressure and bending on this parameter has been estimated. By examining the dielectric characteristics (real and imaginary part of the relative dielectric permeability, tangents from the angle of dielectric losses and conductivity), the possibilities of using the obtained composites as substrates and insulating layers in wireless communication antennas were evaluated.

## II. EXPERIMENTAL PART

### A. Characteristics of the fillers uses – standard kaolin (K) calcined kaolin (CK)

Some of the most important characteristics of the kaolin used are presented in Table 1. All types of kaolin were produced by Kaolin JSC, Bulgaria.

**TABLE I**  
Some of the most important characteristics of the kaolin used

Characteristic Symbol	K	CK1.3	CK1.8	CK4.5
Whiteness, %	-	9.28	89.49	88.98
Wet residue per 45 µm, %	-	0.0026	0.0027	15.46
Particle size(D50), µm (D50 is the diameter at which 50% of a sample's mass is comprised of smaller particles/	7.3	1.3	1.8	4.5
Chemical composition,%				
SiO <sub>2</sub>	max.54.0	58.20	58.20	58.20
Al <sub>2</sub> O <sub>3</sub>	min. 32.0	38.65	38.65	38.65
Fe <sub>2</sub> O <sub>3</sub>	0.70±0.30	0.80	0.80	0.80
TiO <sub>2</sub>	max. 1.2	0.25	0.25	0.25
CaO	max.0.3	-	-	-
MgO	max. 0.2	-	-	-
K <sub>2</sub> O	max.1.4	-	-	-
Na <sub>2</sub> O	max. 0.2	-	-	-
Loss on ignition, %	min. 11.5	0.50	0.50	0.50
Moisture, %	max.1	0.5	0.5	0.5
pH	8±1	7.55	7.55	7.55
Specific density, g/cm <sup>3</sup>	2.60	2.60	2.60	2.60

**B. Formulations of the rubber compounds**

The formulations of the rubber compounds are summarized in Table 2.

**TABLE II**  
Formulations of the rubber compounds used

Ingredients	NR-0	NR-K	NR-CK1.3	NR-CK1.8	NR-CK4.5
Natural rubberSTR 10	100	100	100	100	100
Zinc oxide	3.0	3.0	3.0	3.0	3.0
Filler	0	50	50	50	50
Compatibilizer(Si 69 Silane) (Bis- [3-(triethoxysilyl) propyl]tetrasulfide)	5	5	5	5	5
IPPD(N-Isopropyl-N'-phenyl-1,4-phenylenediamine) Anti-aging agent	1	1	1	1	1
TBBS(N-tert-butyl-benzothiasole-sulfonamide) Vulcanization accelerator	1.5	1.5	1.5	1.5	1.5
Sulfur	2	2	2	2	2

Symbols: NR-0 – virgin compound; NR-K-compound, filled with standard kaolin; NR-CK1.3- compound, filled with calcined kaolin which particles are of D50 = 1.3 micron; NR-CK1.8- compound, filled with calcined kaolin which particles are of D50 = 1.8 micron; NR-CK4.5- compound, filled with calcined kaolin which particles are of D50 = 4.5 microns

**C. Preparation and vulcanization of the test specimens**

The compounds were made on an open laboratory two-rolls rubber mill (L / D 320x160 mm, friction 1.27 and speed of the slower roll 25 min<sup>-1</sup>). The vulcanization of the rubber compounds was carried out on an electrically heated hydraulic vulcanization press with 400x400 mm plates at of 150° C, pressure of 10 MPa and time determined by the vulcanization isotherms of the compounds taken on a MDR 2000 Vulcameter (Alpha Technology). The resulting vulcanisates were plates 150x150x2mm in size.

**D. Characterization methods**

The compounds and the vulcanizates were characterized as follows:

- Vulcanization characteristics - according to BDSISO 3417:2002
- Physicomechanical parameters (Modulus at 100% and 300% elongation, tensile stress, relative elongation, residual elongation) - according to BDS ISO 37:2002 and BDS EN 12 803
- Shore A Hardness– according to BDSISO 7619:2001
- Electrical properties (specific and volume resistivity) according to laboratory methodologies

1. Measurement of the specific volume resistivity  
The specific volume resistivity ( $\rho_v$ ,  $\Omega \cdot m$ ) of flat rubber based specimens in a uniform electric field produced by direct current was calculated by the equation:

$$\rho_v = R_v \cdot S / h \quad (1)$$

where:

$R_v$ - ohmic resistance between the electrodes,  $\Omega$ ;

S - cross sectional area of the measuring electrode,  $m^2$ ;

h – thickness of the sample, m

The ohmic electric resistivity of the composites investigated was measured on a teraohmmeter Teralin III (produced in Germany).

The vulcanizate was placed between two brass electrodes – voltage and measuring with a cross section of  $0.0022 m^2$ . Having switched on the voltage the current running through the sample was allowed to stabilize for 1 min.

2. Measurements of the specific resistivity at varying the applied pressure

The measurements were performed as in item 1. Above, using measuring electrodes which produced pressure upon the samples tested varying as follows: 4; 10; 14.7; 20.6; 25.2; 32.1 and 42.6 kPa.

3. Measuring the specific volume resistivity at varying the bending

The testing set connected to teraohmmeter is presented in Fig. 5. The deformation of the samples subjected to bending was  $1 \div 6\%$ .



Fig. 5. Laboratory set for measuring the specific volume resistivity as a function of bending

(1. Textolite plate; 2. Electrodes; 3. Fixing bolt; 4. Teflon pad for fixing the distance; 5. Steel axis setting the bending degree; 6. Screw for fixing the bending degree; 7. Contact sockets; 8. Test sample)

- Scanning electron microscopy (SEM)

SEM images of the samples tested (virgin and calcined kaolin and the NR-based composites) were taken on a SEM/FIB LYRA I XMU microscope (TESCAN) having the following characteristics: electron source – wolfram heated fiber, resolution –  $3.5 nm$  at  $30 kV$ , acceleration voltage –  $200 V \div 30$

The total pore volume ( $V_t$ ) was determined according to Gurwitsch formula [20] at a relative pressure  $p/p_0 \approx 0.99$ . The volume of the micropores was determined by the  $t$ -method [21], the volume of the mesopores was

$kV$ . An EDXQuantax 200 (Bruker) detector was used to record EDX spectra.

The powder samples of kaolinite were put onto aluminum holders covered by a double-sided carbon tape, which was conductive. Cross sections of the vulcanizate specimens were broken off following the evacuation of the former in liquid nitrogen. The samples thus prepared were covered with carbon in a spray drying chamber.

- Dielectric properties (real  $\epsilon_r'$  and imaginary  $\epsilon_r''$  part of the relative dielectric permittivity, dielectric loss angle tangent  $\tan \delta_\epsilon$  and electrical conductivity  $\sigma$ )  
The dielectric properties of the composite materials were measured by the resonant perturbation method described in a previous publication [17]. According to the resonant perturbation method, the tested sample was introduced into a cavity resonator with dimensions  $61.2 mm \times 10.0 mm \times 610 mm$ . The dielectric parameters of the sample were deduced from the change in the resonant frequency and quality factor of the resonator [17]. For the permittivity measurements the sample was placed at the spot of maximum intensity of electric field, where TE<sub>103</sub> mode was always adopted.

- Determination of adsorption-texture parameters

Low temperature adsorption of nitrogen was used to study the texture of the materials. The adsorption-desorption isotherms were measured on an automated Quantachrome Instruments NOVA 1200e static-volume adsorption apparatus (USA) at  $77.4 K$  and the relative pressure  $p/p_0$  varied  $0.01$  to  $1$ . Prior to adsorption measurements, the samples were degassed under vacuum at  $105^\circ C$  for  $16-18$  hours. The following texture characteristics were calculated: BET ( $S_{BET}$ ) specific surface area, pore total (total) adsorption volume ( $V_t$ ), mean pore diameter ( $D_a$ )  
The specific surface area was calculated using the Brunauer-Emmett-Teller (BET) [18] equation [18]:

$$[W(p_0 - p)] = (1/Wm C) + [(C - 1) / (Wm C)] (p/p_0), (2)$$

where  $Wm$  is weight of the gas, needed for the formation of a monomolecular layer,  $p/p_0$  – relative pressure;  $W$  – weight of the adsorbed gas;  $C$  – energy constant. The value of the specific surface area  $S_{BET}$  is calculated by the formula

$$S_{BET} = w \cdot Wm \cdot N_A, (3)$$

where  $N_A$  – Avogadro's number,  $w$  – the surface occupied by a molecule of adsorbate in a full monolayer. For nitrogen  $w = 0.162 nm^2$  [19].

the difference between the total pore volume ( $V_t$ ) and the micropores. The size distribution of the pores was made by the method of Barrett-Joyner-Halenda (BJH) [22].

III. RESULTS AND DISCUSSION

A. Characterization of the fillers used

The particles of the fillers used were characterized by scanning electron microscopy(Fig. 6).

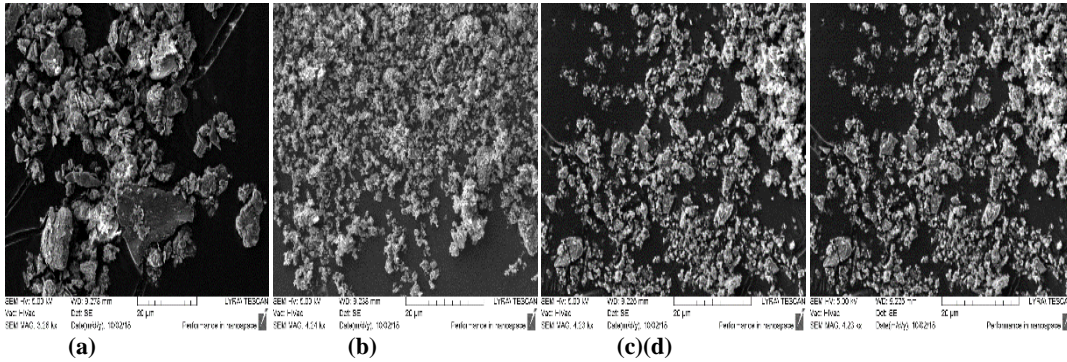


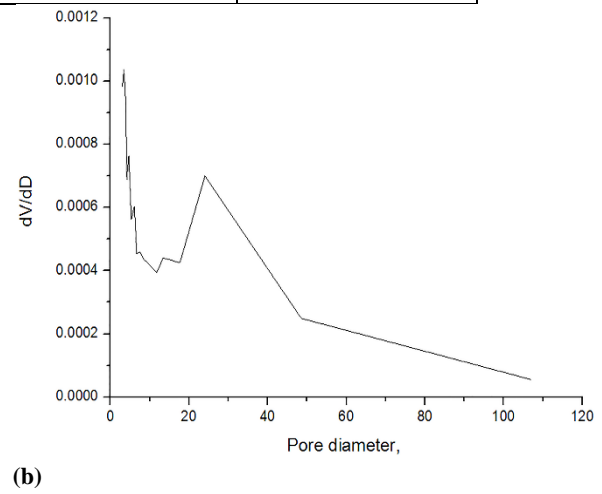
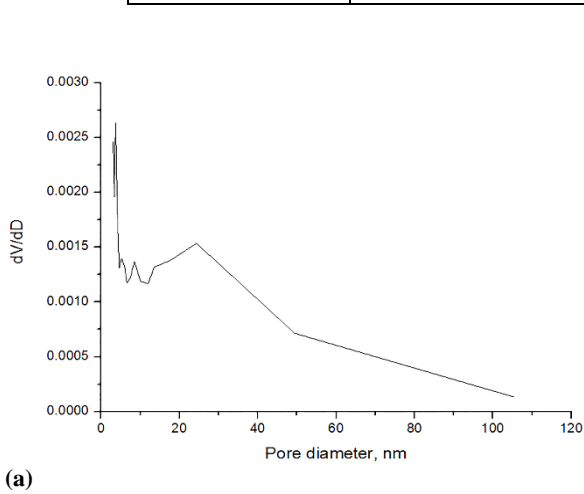
Fig.6.SEM images of virgin kaolin (a) and calcined kaolin with a particle D50 of 1.3 microns (b), 1.8 microns (c) and 4.5 microns (d)

The difference in the particle size is obvious, as can also be seen from the markers placed on the images showing the micron size of some of the more particle-shaped and particle size. The particles of virgin uncalcined kaolin are significantly larger than those of the calcined ones. The large particle size

dispersion of uncalcined kaolin, in which particles of 1 to 25 microns observed is also noteworthy. In the calcined kaolin the dispersion in the particle size is considerably smaller. The adsorption-texture characteristics of the studied fillers are summarized in Table 3, and Fig. 7 shows the pore size distribution.

TABLE III  
Adsorption-texture characteristics of the fillers studied

Sample	$S_{BET}$ , $m^2/g$	$V_t$ , $cm^3/g$	$D_{av}$ nm
K st	18	0.08	17
CK 1.3	9	0.04	16
CK 1.8	8	0.03	14
CK 4.5	6	0.01	7



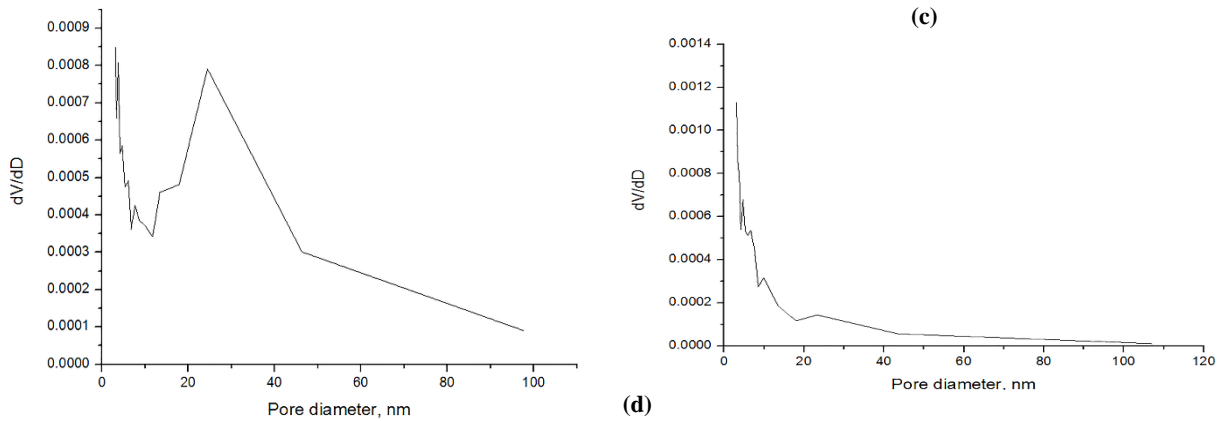


**Fig.7. Pore size distribution: (a) standard kaolin, (b) calcined kaolin with D50=1.3; (c) calcined kaolin with D50 =1.8; (d) calcined kaolin with D50=4.5**

Table 3 shows the serious changes occurring in the kaolin structure during its calcination. The standard kaolin, which has the largest particle size, also has the highest specific surface area, obviously due to its pores, which have the highest total volume and greatest average diameter. According to the IUPAC classification [23], porous materials, depending on the size of their pores, are divided into 3 main classes: microporous (<2nm); mesoporous (2-50nm); macroporous(>50nm). Obviously, in the case of standard kaolin, the mesopores (Fig. 7a) predominate.

During the calcination of kaolin, with the increase of the particle size D50, the specific surface, the total volume of the pores and their average diameter decrease, in the case of CK4.5 the decrease is significant (Table 3). It is noteworthy that in calcination of kaolin, although the particle size decreases compared to the standard, the specific surface does not increase, but also decreases. That is obviously due to the destruction of the porous structure of standard kaolin and the change in the ratio of the pores of the calcination, as seen from the comparison of Fig. 7, a-d. Pores definitely diminish, mesopores too.

**B. Vulcanisation characteristics of mixtures containing standard and calcined kaolin**

The vulcanization characteristics of the tested composites are shown in Table 4. The results in Table 4 show that the minimum torque, which is often associated with the effective viscosity of the mixture, is practically not influenced by the

type of kaolin. By contrast, the maximum torque (often associated with the rigidity of the mixture) and the difference  $\Delta M = MH-ML$  (associated with the density of the vulcanization network) are strongly affected by calcination, increasing almost twice compared to the values of the compounds with standard uncalcinated kaolin. It is also notable that with the increase in the calcined kaolin particles D50 from 1.3 to 4.5 microns, the values of these characteristics also increase. The tendency to premature vulcanization of the compounds with calcined kaolin, as assessed by  $t_{s1}$  and  $t_{s2}$  characteristics, is increasing compared to that of the compounds containing uncalcinated kaolin.

With the increasing particle size this trend is increasing ( $t_{s1}$  and  $t_{s2}$  decreasing). The values of the tangent of of mechanical loss angle at the minimum and maximum torque decreases as a result of calcination but the particle size of the calcined kaolin does not practically affect them. The time to carry out 50% of the curing process is reduced both as a result of calcination and of larger particle size of calcined kaolin. The optimal curing time ( $t_{90}$ ) for the calcined kaolin increases significantly, with a particle size increase showing a downward trend.

In conclusion, the calcination of kaolin has a noticeable effect on almost all the vulcanization characteristics of the compounds based on natural rubber containing if compared to those of the compounds containing uncalcinated kaolin.

**TABLE IV  
Vulcanization characteristics at 150 °C**

Characteristics	NR-0	NR-K	NR-CK1.3	NR - CK1.8	NR – CK4.5
ML, dN.m	0.17	0.09	0.08	0.08	0.08
MH, dN.m	4.92	5.83	9.31	9.62	10.05
$\Delta M=MH-ML$	4.75	5.74	9.23	9.54	9.97
$t_{s1}$ , m:s	7:36	9:43	7:38	7:24	6:54
$t_{s2}$ , m:s	8:10	10:22	8:01	7:48	7:16

tand@ML	1.177	2.000	1.625	1.750	1.750
tand@MH	0.020	0.030	0.014	0.014	0.013
T <sub>50</sub> , m:s	8:24	9:43	8:58	8:43	8:12
t <sub>90</sub> , m:s	11:51	10:22	15:08	14:41	14:12

Symbols:

ML (minimum torque), MH (maximum torque), ΔM = MH-ML, T<sub>50</sub> (optimal time for completion of 50% vulcanization); T<sub>90</sub> (optimal time to complete 90% curing), t<sub>s1</sub> (scorch time estimated as an increase in the torque by one unit), t<sub>s2</sub> (scorch time, estimated as an increase in the torque by two units); tand @ ML (tangent of mechanical loss angle at minimum torque); tand @ MH (tangent f mechanical loss angle at maximum torque).

**C. Physico-mechanical characteristics**

The physico-mechanical characteristics of the studied composites are summarized in Table 5. As Table 5 shows, the calcination of kaolin leadsto a significant decrease of M<sub>100</sub> values of the vulcanizates and while of those for M<sub>300</sub>, especially, of the calcined kaolin having particle size D5=1.3 microns – the decrease is negligible. As the particle size increases, the values of this parameter decrease as a rule. The same trend is seen in the tensile strength. The calcination (with the exception of the composite containing calcined kaolin with a particle D50 of 4.5 microns) does not practically affect the relative elongation. The residual elongation in the calcined

kaolion (D50=1.3 and D50=1.8 microns) is much lower at the same or even higher values of the relative elongation, which is indicative of a somewhat improved elasticity of the vulcanisates. Shore A hardness as a result of calcination increases. Amongst the calcined kaolins, that having particles of D50=1.3 microns exhibits the best physico-mechanical performance.

When trying to explain these results, one should keep in mind that the virgin natural rubber is a crystallizing elastomer with a pronounced tendency to self-reinforce as a result of the existing crystallites in its volume, acting as active fillers. Therefore, there is no reinforcement effect - the addition of any kaolin

**TABLE V**  
**Physico-mechanical characteristics of the studied composites**

Characteristics	NR-0	NR-K	NR-CK1.3	NR-CK1.8	NR-CK4.5
Modulus at 100% elongation, M <sub>100</sub> , MPa	0.2	1.6	0.7	0.7	0.7
Modulus at 300% elongation, M <sub>300</sub> , MPa	0.7	7.4	7.0	6.5	5.5
Tensile strength, σ, MPa	19.0	17.2	16.7	16.0	8.0
Relative elongation, ε <sub>rel</sub> , %	900	500	550	500	350
Residual elongation, ε <sub>res</sub> , %	5	35	15	15	10
Shore A Hardness, rel. units	44	57	60	60	60

leads to a decrease of the performance compared to that of non-filled vulcanizates. Obviously, here the sense of filling is in lowering the cost of the material.

There are two interactions affecting the vulcanization characteristics as well as the reinforcement - "rubber-

filler" and "filler-filler". It can be assumed that as a result of the calcination the surface the particles has less active functional groups (such as hydroxyl ones). As well as due to particle size decrease and to the increase in their surface, the interaction of rubber-filler is weakened, but the filler-filler interaction is enhanced. The lack of active functional groups on the surface of the calcined kaolin also impedes the functioning of the bifunctional compatibilizers of silane type, so the effect of their presence in the rubber mixtures is not very well expressed. Additional light on the influence of standard and calcined kaolin on the physical-mechanical characteristics gives the adsorption-texture characteristics (Table 3, Fig.7).

Obviously of the greatest importance for the reinforcing effect are the mesopores which provide a high specific surface and have a suitable diameter for penetration of rubber macromolecules and provide sufficient contact spaces between them and the surface of the filler. The strong "rubber-filler" interaction ensures good physical-mechanical performance. In calcined kaolin, as a result of the breakdown of the original structure, the specific surface, the total volume and the pore diameter decrease, the mesopore mass decreases significantly. All that limits the macromolecules access of to the surface of the fillers and the possibilities for contact between them, therefore weakening of the rubber-filler interaction and worsening of the physical-mechanical parameters. One more conclusion can be made: uncalcined kaolin has the largest particle size and the largest dispersion in size but is also the richest in active functional groups. Calcined kaolin has a smaller particle size, but the latter are poorer to active groups that have been removed by calcination. Obviously, in this case, the presence of functional groups on the surface of the

filler contributing to enhanced "rubber-filler interaction" appears to be a more important factor than the decrease of particle size. Hence, composites with calcined kaolin is somewhat inferior to the uncalcine one.

**D. Electrical Properties**

The electrical properties of the composites studied and their dependence on the chemical nature and particle size of the fillers used, the applied external pressure and the degree of bending are shown in Fig. 8-10.

The results of the studies show (Fig. 8) that the samples containing standard kaolin have a higher resistance than the samples containing calcined kaolin, with increasing the D50 of the particles of the latter, the resistance also increases. All filled composites have a higher resistance than those of the virgin ones. The behavior of varying specific impedance by increasing the pressure on the sample within the range of 0-45 kPa varies depending on the type of filler (Fig. 9).

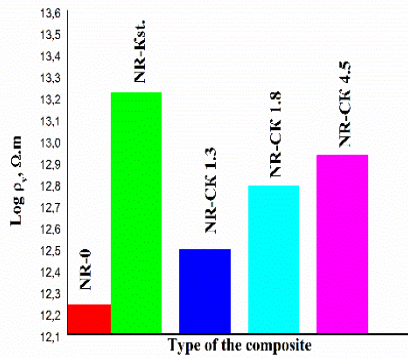


**Fig.8.** Dependence of the specific volume electrical resistance on the chemical nature and particle size of the filler (the symbols for the composites used are given after Table 2).

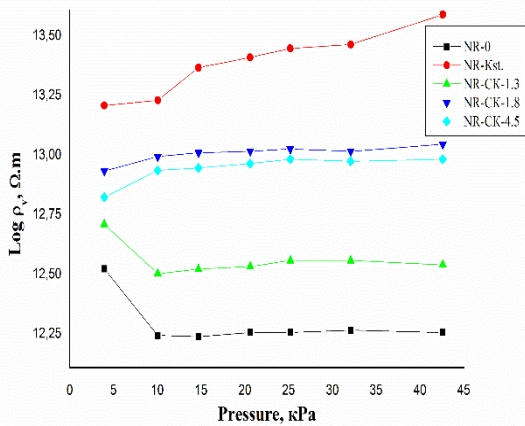


**Fig.9.** Dependence of the specific volumetric electrical resistance on the external pressure applied to the samples at the time of measurement (the symbols for the composites used are given after Table 2).

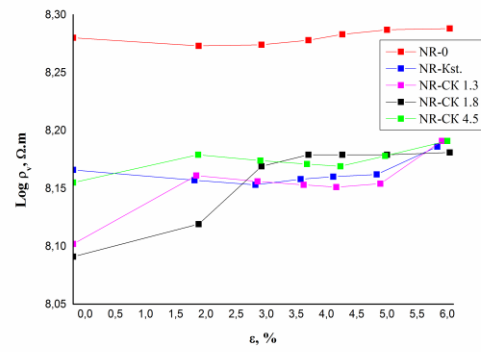


**Fig.10.** Dependence of specific volume electrical resistance on the bending degree ( $\epsilon$ ) of the samples at the time of measurement (the symbols for composites used are given after Table 2).

In the virgin composite and the one containing calcined kaolin with particles of D50=1.3 microns with a pressure increase, the resistance initially decreases, then retains an almost constant value. In the composites containing calcined kaolins with particles of D50=1.8 and 4.5 microns with increasing pressure, the resistance initially increases, then retains an almost constant value. In the composite containing standard kaolin, with the increasing pressure, the resistance increases in the whole range examined. In this case, the samples with standard kaolin have the highest resistance, and the lowest is for the virgin composites.

As the degree of bending increases, the resistance of the composites generally tends to increase, but their behavior is different and different subareas can be defined (Fig. 10). For calcined kaolins, one primary area (bending can be defined within the range of 2.0-2.5%) wherein the resistance increases; after that, another area (bending about 5%) is observed, where the resistance remains relatively constant, followed by a third area in which the bending increases again. In the case of virgin composites and those containing standard kaolin, the course of dependence is slightly different: after initially very slight decrease of the resistance (to about 3.0-3.5%), it starts to increase slightly, as for the composite with standard kaolin, this effect is better expressed. It is noteworthy that here, unlike previous dependencies, the virgin composite has the highest resistance, and almost in the entire investigated range (bending over 2.5%), the composites with calcined kaolin (particles of D50= 4.5 and 1.8 microns) have a higher resistance than the composites containing standard kaolin.

It can be assumed that in the dielectric matrix of natural rubber the conductivity occurs by an ionic mechanism. The images obtained by scanning electron microscopy (Fig. 11) show that in all the cases investigated there is a uniform distribution of the particles of the filler particles in the rubber matrix, reduction of the space between the particles in the reduction of their size and increase of these distances with increasing the size (compare Fig. 11c with 11d and 11e). Noteworthy is that the studied composites



obviously have a wide variety of different ions: calcination releases bound water (associated with  $H^+$  and  $OH^-$  ions transport), SEM-EDX /spectroscopy on scanned electronic microscopy, showed the presence of iron, potassium, titanium ions in the calcined kaolins missing in some areas of standard uncalcined kaolin (Fig. 12a), which may explain the resistance of composites with calcined kaolins which is the lower than that of the composites with standard kaolin, more so in some areas of the calcined kaolin (Fig.12d/ concentration of these ions is 2-3 times (compare Fig.12b). In any case, the effect on the resistance is the distance between the charge carriers, which changes with the change in particle size at the same degree of filling (at a smaller particle size the distance between the carriers is smaller and the resistance decreases and vice versa); the distance between the charge carriers are also changed when the applied pressure on the sample changes as well as with its bending: in the first case they are reduced and in the second they increase. Studies with the SEM-EDX (Fig. 12) also show a large variation in the elemental composition of the studied areas in kaolin particles - both in uncalcined and calcined kaolin, which reveals both uneven concentration of charge carriers and for drastic changes, occurring with the calcination process. The ratio between all factors influencing the volume resistance also determines the overall behavior of the composite depending on the dominant influence of one or another factor.

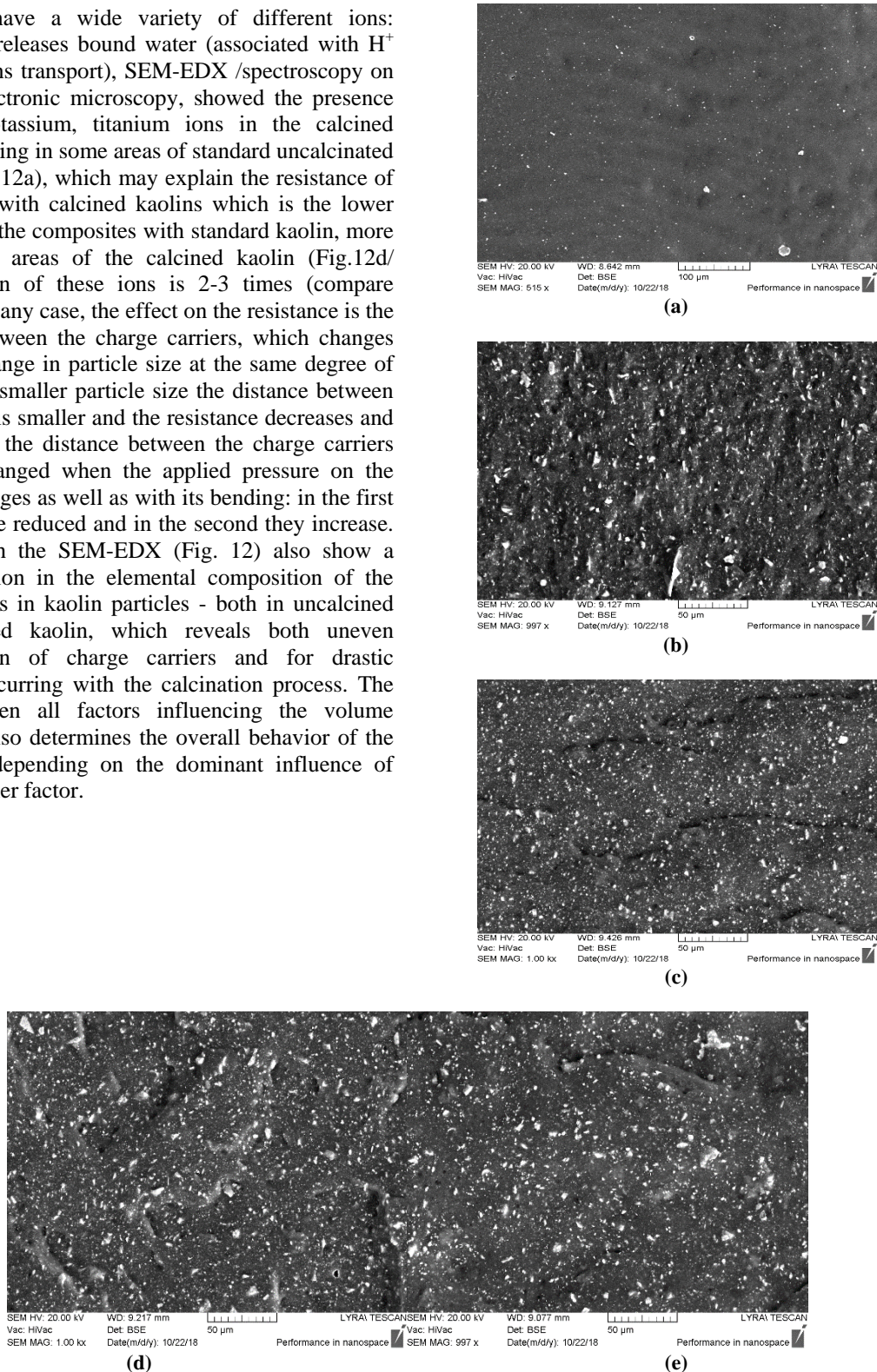


**Fig.11.SEM images of the studied composites:(a) virgin; (b) filled with standard kaolin; (c) filled with calcined kaolin with a particle size of  $D_{50}=1.3$  microns; (d) filled with calcined kaolin with a particle size of  $D_{50}=1.8$  microns; (e) filled with calcined kaolin with a particle size of  $D_{50}=4.5$  microns.**

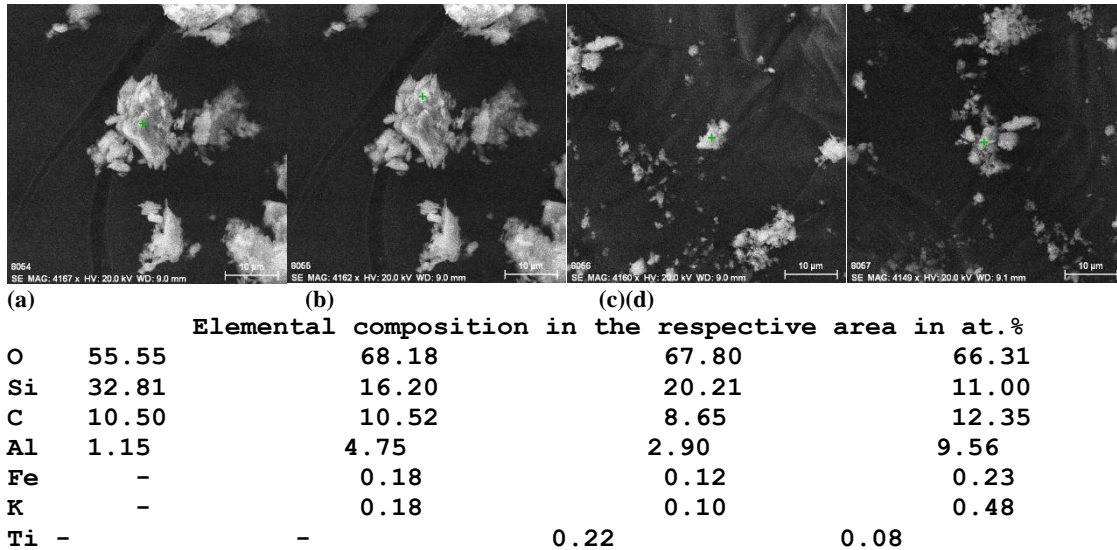


**Fig. 12. Results from the elemental composition analysis (in at. %) in various areas of the investigated fillers performed by energy-scattering X-ray spectroscopy on scanning electron microscopy (SEM-EDX). A cross is the area where the X-ray diffraction spectroscopy is performed.**

(a) standard kaolin - area 1; (b) standard kaolin - area 2; (c) calcined kaolin with a particle size of D50=4.5 microns - area 1; (d) calcined kaolin with a particle size of D5 =4.5 microns - area 2

**Dielectric characteristics**

Table 6 presents the real ( $\epsilon_r'$ ) and imaginary ( $\epsilon_r''$ ) part of the relative dielectric permittivity, tangent of dielectric loss angle and electrical conductivity of NR-based vulcanizates containing standard and different types of calcined kaolin at 2.56 GHz.

The results in Table 6 show that with increasing the particle size D50 of calcined kaolin, all the measured dielectric characteristics of the composites at the used frequency gradually increase, but overall (with the

exception of  $\epsilon_r'$ ) they remain lower than the corresponding parameters of the composites with uncalcined kaolin. These results are due to the fact that the dielectric losses in a multiple composite are the result of complex phenomena such as natural resonance, dipole relaxation, electronic and interfacial polarization. Interfacial polarizations occur in heterogeneous media due to the accumulation of charges at the interfaces and the formation of large dipoles [24].

**TABLE VI**  
**Dielectric characteristics of natural rubber based composites**

f=2565.355 MHz	$\epsilon_r'$	$\epsilon_r''$	$\sigma, S/m$	$\tan\delta_\epsilon$
NR-0	2.75108822	0.006041	0.000862	0.002196
NR-K	2.4561007	0.005469	0.00078	0.002132
NR-CK1.3	2.74026617	0.000355	0.0000507	0.00013
NR-CK1.8	2.77522934	0.00312	0.000445	0.001068
NR-CK4.5	2.87871108	0.005326	0.00076	0.00185

The important factor is also the ratio between the particles of the fillers and the host materials [25]. The morphology and structure of the used filler, the changes occurring during the calcination, the differences in particle size and shape, as well as the differences in the morphology, structure and composition of the composite affect the changes in the real and imaginary part of the relative permittivity. The above is confirmed by the data in Fig. 13, which presents the results of SEM-EDX studies on the composites, as well as those containing uncalcined

and calcined kaolin with a D50=4.5 microns. The figure shows the significant difference in the composition of the composites, which in itself is the reason for the differences in the studied characteristics. In virgin composites, the carbon from natural rubber dominates naturally, with 84.32 at. %, and oxygen is 14, 46 at. %. In the composite with uncalcined kaolin this ratio is 55.66: 36.38 at.%, And in the composite containing calcined kaolin with a D50=4.5 micron it is 61.40: 29.01 at. %, most likely due to the separation in the calcination of the hydroxyl groups of the kaolin structure (Fig. 2-3) associated

also with changes in its composition. Differences between composites with uncalcined and calcined kaolin are also observed in the amounts of other elements. That indicates that changes actually occur in the composition of the composite, which also explains differences in dielectric characteristics.

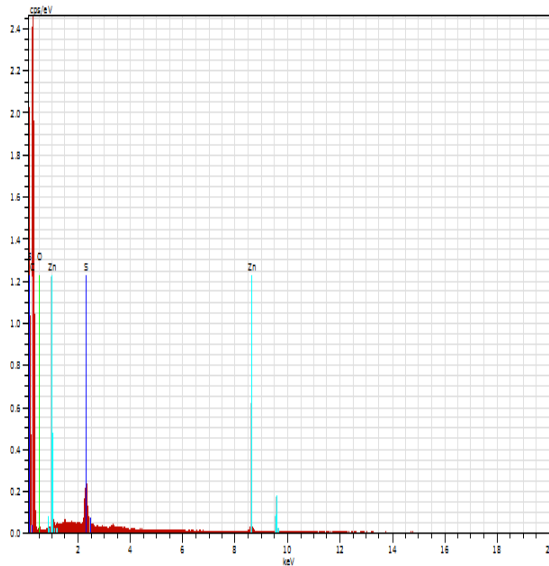
The requirements and typical features of **the rubber substrate antenna material** may be summarized as follows [26, 27]:

-Relative dielectric constant ( $\epsilon'$ ) can be selected arbitrarily (2-20). According to other authors, the dielectric constant of the various flexible substrates is in the range of 2.2-12.0 [28]. The lower dielectric constant declines the surface wave losses which are related to the guided wave broadcast within the substrate [29].

-Low dielectric loss tangent (0.01 or lower)

Loss tangent ( $\tan\delta$ ) is also identified as a dissipation factor. It describes the amount of power turned into heat in the substrate material. The loss tangent in the following relation is defined as the ratio of the imaginary part to real part of the relative permittivity. The higher values of loss tangent results in additional losses in the dielectric substrate and higher losses outcomes in reduced radiation efficiency [30].

From the results presented in Table 6 and from the above-mentioned requirements to the materials used as antenna pads, it can be seen that the composite containing calcined kaolin with a particle size  $D_{50}=1.3$  (NR-CK1.3) is highly suitable for antenna applications. That is why, the value of  $\epsilon'$  at a frequency of 2.565 GHz is 2.7402, and that of  $\tan\delta_c$  - 0.00013, i. it is much lower than the values of all other composites studied.



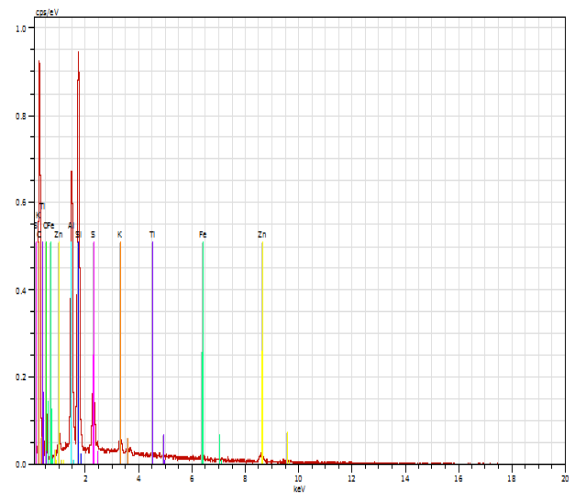
a)

NR 0

El	AN	Series	unn. C [wt.%]	norm. C [wt.%]	Atom. C [at.%]	Error [%]
----	----	--------	---------------	----------------	----------------	-----------

C	6	K-series	77.98	77.98	84.32	24.2
O	8	K-series	17.82	17.82	14.46	6.9
S	16	K-series	1.83	1.83	0.74	0.1
Zn	30	K-series	2.38	2.38	0.47	0.1

Total: 100.00 100.00 100.00



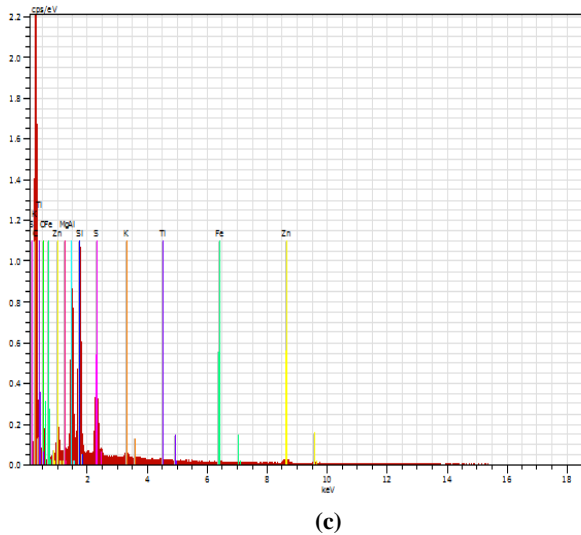
(b)

NR-K

El	AN	Series	unn. C [wt.%]	norm. C [wt.%]	Atom. C [at.%]	Error [%]
----	----	--------	---------------	----------------	----------------	-----------

C	6	K-series	44.86	44.86	55.66	16.9
O	8	K-series	39.05	39.05	36.38	70.7
Si	14	K-series	6.49	6.49	3.44	0.3
Al	13	K-series	5.57	5.57	3.08	0.3
S	16	K-series	1.73	1.73	0.81	0.1
Zn	30	K-series	1.23	1.23	0.28	0.1
K	19	K-series	0.52	0.52	0.20	0.0
Fe	26	K-series	0.36	0.36	0.10	0.0
Ti	22	K-series	0.18	0.18	0.06	0.0

Total: 100.00 100.00 100.00



NR-K4.5

El	AN	Series	unn. [wt.%]	C norm. [wt.%]	Atom. [at.%]	Error [%]
C	6	K-series	49.26	49.26	61.40	17.8
O	8	K-series	31.00	31.00	29.01	51.3
Si	14	K-series	6.59	6.59	3.51	0.3
Al	13	K-series	6.15	6.15	3.41	0.3
S	16	K-series	3.51	3.51	1.64	0.2
Zn	30	K-series	2.33	2.33	0.53	0.1
Mg	12	K-series	0.39	0.39	0.24	0.1
K	19	K-series	0.30	0.30	0.11	0.0
Ti	22	K-series	0.22	0.22	0.07	0.0
Fe	26	K-series	0.25	0.25	0.07	0.0
Total:			100.00	100.00	100.00	

Fig.13. EDX spectra and their composite element composition data as follows: (a)virgin; (b) filled with uncalcinated kaolin; (c) filled with calcined kaolin with particle size D50 - 4.5 microns.

The composite is also characterized by a minimal absorption of electromagnetic power and a good balance of physico-mechanical properties.

The antenna consists of a multilayer substrate (1-3) of a composite comprising kaolin which particle size D50 is 1.3(NR-CK1.3), a feeding strip line (4), a modified planar dipole antenna (5), two meandered lines (6) to generate dual resonance modes and a rectangular reflector (7), as is shown in Fig. 14.

The metal components of the antenna are made of 0.05 mm thick copper foil for the radiating elements and 0.011 mm thick aluminum foil for the reflector. The studies have shown that the elastomeric composition NR-CK1.3 used as insulating layers and a substrate in the flexible antenna provides the following advantages:

1. High radiation efficiency when placed in a free space or on / in close proximity to a flat homogeneous human body model with electromagnetic parameters approaching those of human muscle; Fig. 15-16;

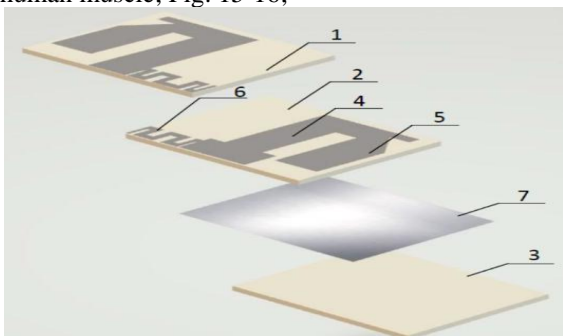


Fig.14. Structure of the antenna containing compositeNR-CK1.3:amultilayersubstrate(1-3), afeedingstripline (4), modifiedplanardipoleantenna (5), twomeanderedlines(6), arectangularreflector(7).

As seen from the figures, at a frequency of 2.6 GHz, the maximum efficiency of the antenna radiation in the free space is 64.19% and on the human body model is 50.85%. At a frequency of 5.6 GHz, the maximum antenna radiation efficiency in the free space is 73.82%, and on a human body model is 44.20%. By comparison, at a frequency of 2.6 GHz when the substrate layers are based on a virgin NRB-based composite [31], the maximum emission efficiency in the free space decreases to 34.74% and that on a human body model to 26.51%. At a frequency of 5.6 GHz, the maximum emitting efficiency of the composite based on acrylonitrile butadiene rubber in the free space decreased to 44.06% and on a human body model to 26.81%. As seen from the results in Fig. 15-16, the efficiency of the antenna with a pad of multilayer composite filled with calcined kaolin of particle size D50 1,3(NR-CK1.3) remains high in both the 2.4-2.7 GHz (Fig. 15) and the 5.24-5.84 GHz (Fig. 16) bands.

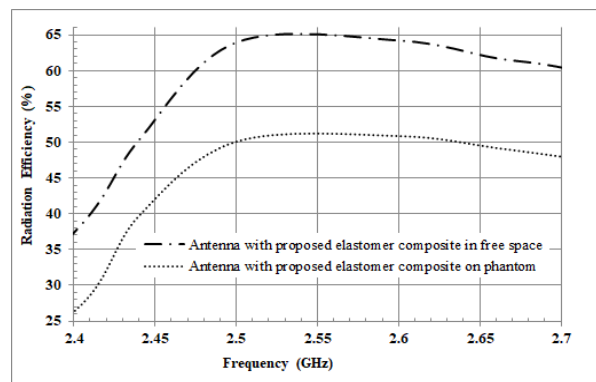


Fig. 15. Emission efficiency of an antenna with insulating layers and substrate of a composite NR-CK1.3 in the 2.4-2.7 GHz frequency range

2. High values of the antenna gain coefficient due to minimal absorption of electromagnetic power in the composite (Fig.17-18).

The figures show that the maximum amplification coefficient of the multilayer antenna of composition NR-CK1.3 in the range 2.4-2.7 GHz in the free space is 4.23 dBi and when the antenna is placed on a model of the human body - 4.59 dBi. In the 5.24-5.74 GHz frequency range, the maximum gain in the free space is 3.38 dBi, while the human body model is 2.39 dBi. Comparing the data with those from [31] one sees that when the substrates are made of a nitrile butadiene rubber (NBR) based composite, the amplification coefficients in the 2.4-2.7 GHz range are 1.47 dBi and 1.64 dBi, respectively, and in the frequency range 5.24-5.74 GHz, 1.20-1.09 dBi, respectively.

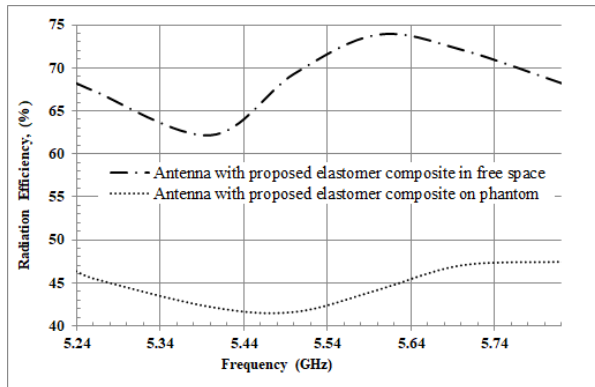


Fig. 16. Emission efficiency of an antenna with insulating layers and substrate of a composite NR-CK1.3 in the 5.24-5.74 GHz frequency range

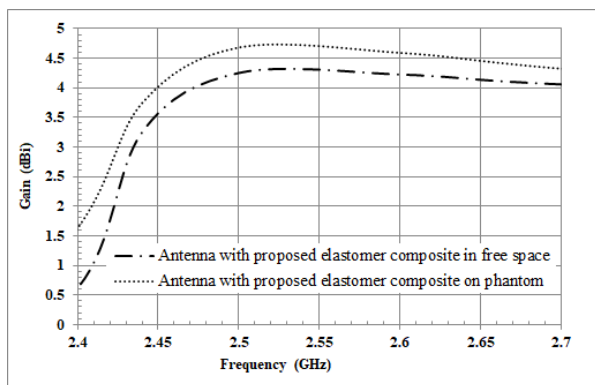


Fig. 17. Antenna amplification coefficients with insulating layers and substrate of a composite NR-CK1.3 in the frequency range 2.4-2.7 GHz

3. Good balance of electromagnetic parameters (low variation of complex dielectric permeability) in a wide frequency range.

Concerning the good balance of electromagnetic properties in the wide frequency range, allowing good coordination of the antenna are presented in Fig. 19 results for reflection coefficient from the input of the antenna when placed in free space or on / in

close proximity to a flat homogeneous human body model.

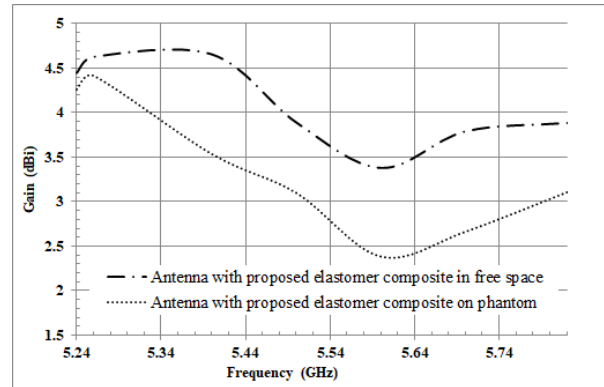


Fig. 18. Antenna amplification coefficients with insulating layers and substrate of a composite NR-CK1.3 in the frequency range 5.24-5.74 GHz

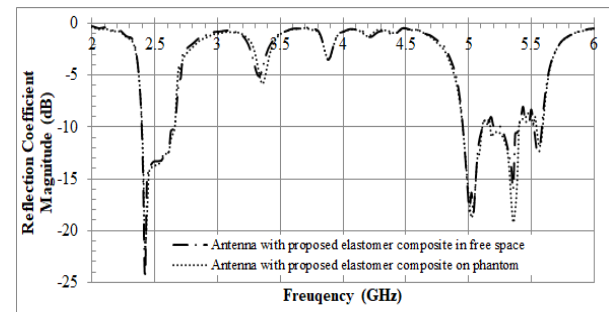


Fig. 19. Reflection coefficient modulus of the antenna input containing as insulating layers and substrate of a composite NR-CK1.3 when placed in a free space or on / in close proximity to a flat homogeneous human body model.

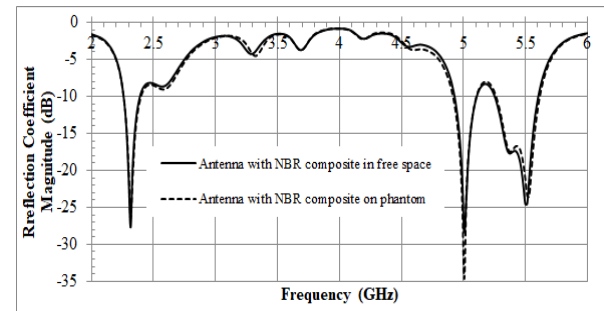


Fig. 20. Reflection coefficient modulus at the entrance of the antenna containing, as insulating layers and substrate, a NBR-based composite when placed in a free space or on/adjacent to a flat, human body model.

By comparing the results shown in Fig. 19 and 20, one sees that the multilayer antenna of the described elastomer composition has better matching in the frequency ranges of 2.4-2.7 GHz and 5.1- 5.4 GHz compared to cases where the substrate layers are of a composition based on unfilled nitrile butadiene rubber NBR [31]. A -10 dB  $|S_{11}|$  reference level (Voltage Standing Wave Ratio -VSWR  $\leq 2$ ) is used to define impedance bandwidths. As can be seen from Fig. 19 in the free space and on a phantom the antenna with a multilayer substrate of the NR-CK1.3 composition shows the simulated bandwidth of 260 MHz (2.4-2.66 GHz) and 690 MHz (4.9-5.59 GHz) at

lower and higher band, respectively. The comparison with the antenna described in [31], wherein the multilayer pad is of a acrylonitrile butadiene rubber reveals the simulated bandwidth of 170 MHz (2.25-2.42 GHz) and 510 MHz (4.92-5.10 GHz and 5.28-5.61) at a lower and higher band, respectively.

#### IV. CONCLUSIONS

The impact of standard uncalcined kaolin and calcined kaolin with different D50 values of its particles on the vulcanization, physico-mechanical, electrical and dielectric properties of NR-based composites has been compared.

A significant influence of the changes occurring with the calcination of kaolin as well as of the particle size on all tested properties has been found. Therefore, composites containing uncalcined and calcined kaolins vary greatly. It can be categorically stated that the observed differences are due to the profound structural changes and the changes in the elemental composition occurring in the kaolin during the process of its calcination, and the influence of these changes on the factors influencing most strongly the studied properties ("rubber- filler" and " filler-filler "interactions, concentration of ions of various chemical elements, etc.). From the point of view of antenna applications, it can be asserted that the composite containing calcined kaolin with particles of D50=1.3 is the most suitable since it has an extremely low tangent of the dielectric loss angle and provides the best antenna- high efficiency of radiation, high gain, good balance of electromagnetic properties in a wide frequency range.

#### ACKNOWLEDGMENT

The authors would like to acknowledge the support of King Khalid University for this research through a grant # RCAMS/KKU/006-18 under the Research Center for Advanced Materials Science at King Khalid University, Saudi Arabia and that of the University of Chemical Technology and Metallurgy, Sofia, Bulgaria.

The authors also appreciate the calcined kaolin samples provided kindly by Kaolin Ltd. Bulgaria.

#### REFERENCES

- [1] C.D. Dimitrakopolous, C.D. and P.R.L. Malenfant, "Organic Thin Film Transistors for Large Area Electronics", *Adv. Mater.*, vol. 14, pp.99-117, 2002.
- [2] R. Morent, N. De Geyter, F. Axisa, N. De Smet, L. Gengembre, E. De Leersnyder, et al. "Adhesion enhancement by a dielectric barrier discharge of PDMS used for flexible and stretchable electronics", *J. Phys. D: Appl. Phys.*, vol. 40, pp.7392 -7401, 2007.
- [3] J.D. Bolt, D.P. Button, and B.A. Yost, "Ceramic-fiber—Polymer composites for electronic substrates", *Mater. Sci. Eng: A*, vol. 109, pp. 207-211, 1989.
- [4] I.J. Youngs, G.C. Stevens, and A.S. Vaughan, "Trends in dielectrics research: an international review from 1980 to 2004", *J. Phys. D: Appl. Phys.*, vol. 39, pp.1267-1276, 2006.
- [5] M.T. Sebastian, and H. Jantunen, "Polymer–Ceramic Composites of 0–3 Connectivity for Circuits in Electronics: A Review", *Int. J. Appl. Ceram. Technol.*, vol. 7, pp. 415-434, 2010.
- [6] H. Ohsato, T. Tsunooka, T. Sugiyama, K. Kakimoto, and H. Ogawa, "Forsterite ceramics for millimeterwave dielectrics", *J. Electroceram.*, vol. 17, pp. 445-450, 2006.
- [7] M.T. Sebastian, (2008). *Dielectric materials for wireless communication*, Oxford, UK: Elsevier Publishers, 2008.
- [8] K.P. Surendran, N. Santha, P. Mohanan, P. and M.T. Sebastian, "Temperature stable low loss ceramic dielectrics in (1-x)ZnAl<sub>2</sub>O<sub>4</sub>-xTiO<sub>2</sub> system for microwave substrate applications", *Eur. Phys. J. B*, vol. 41, pp. 301-306, 2004.
- [9] S. Rimdusit, and H. Ishida, "Development of New Class of Electronic Packaging Materials Based on Ternary Systems of Benzoxazine, Epoxy, and Phenolic Resins", *Polymer*, vol. 41, pp.7941-7949, 2000.
- [10] D.P. Button, B.A. Yost, R.H. French, W.Y. Hsu, J.D. Belt, M.A. Subrahmanian, et al. "Ceramic substrates and packages for electronic applications", *Advances Ceramic*, American Ceramic Society, Westerville OH, vol. 26, pp. 353-373, 1989.
- [11] E.M. Dannenberg (1982). "Filler Choices in the Rubber Industry", *Rubber Chem. Technol.*, vol. 55, pp. 860-880, 1982.
- [12] T.D. Kelly, and G.R. Matos, (2005) "Historical Statistics for Mineral and Material Commodities in the United States", US Geological Survey, Data Series 140
- [13] W. Waddell, and L. Evans, "Use of Nonblack Fillers in Tire Compounds", *Rubber Chem. Technol.*, vol. 69, pp. 377-423, 1996.
- [14] E. Gerasimov, *Ceramic Technology*, Sofia, Bulgaria: Saraswati, 2003.
- [15] Huber Engineered Materials, *Ingredients for Rubber Reinforcement*, [Online] Available: [www.hubermaterials.com/215htm](http://www.hubermaterials.com/215htm)
- [16] M. Hancock, "Mineral additives for thermal barrier plastics film", *Plasticulture*, vol. 79, pp. 4-14, 1988.
- [17] A.A. Al-Ghamdi, O.A. Al-Hartomy, F.R. Al-Solamy, N.T. Dishovsky, P. Malinova, N.T. Atanasov, and G.L. Atanasova, "Conductive Carbon Black/Magnetite, Hybrid Fillers in Microwave Absorbing Composites Based on Natural Rubber", *Compos. Part B-Eng.*, vol. 96, pp.231-241, 2016.
- [18] S. Brunauer, P.H. Emmett, and E. Teller, "Adsorption of Gases in Multimolecular Layers", *J. Am. Chem. Soc.*, vol. 60, pp. 309-319, 1938.
- [19] I. Ismail, "Cross-sectional areas of adsorbed nitrogen, argon, krypton, and oxygen on carbons and fumed silicas at liquid nitrogen temperature", *Langmuir*, vol. 8, pp. 360–365, 1992.
- [20] S. Lowell, J. Shields, M.A. Thomas, and M. Thommes, *Characterization of Porous Solids and Powders: Surface Area, Pore Size and Density*, Netherlands: Springer, 2004.
- [21] J.H. de Boer, B.G. Linsen, T.H. van der Plas, and G.J. Zondervan, "Studies on pore systems in catalysts: VII. Description of the pore dimensions of carbon blacks by the t method", *J. Catal.*, vol. 4, pp. 649-653, 1965.
- [22] E.P. Barrett, L.G. Joyner, and P.P. Halenda, K.S.W. "The Determination of Pore Volume and Area Distributions in Porous Substances. I. Computations from Nitrogen Isotherms", *J. Am. Chem. Soc.*, vol. 73, pp. 373–380, 1951.
- [23] K.S.W. Sing, D.H. Everett, R.H.W. Haul, L. Moscou, R.A. Pierotti, J. Rouquerol, and T. Siemieniowska, "Reporting Physisorption Data for Gas/Solid Systems with Special Reference to the Determination of Surface Area and Porosity", *Pure Appl. Chem.*, vol. 57, pp. 603-619, 1985.
- [24] M. Mirsha, A.P. Singh, P. Sambyal, S. Teotia, and S.K. Dhawan, "Facile synthesis of Phenolic Resin Sheet Consisting Expanded Graphite/-Fe<sub>2</sub>O<sub>3</sub>/SiO<sub>2</sub> Composite and Its Enhanced Electromagnetic Interference Shielding Properties", *Indian J. Pure Ap. Phy.*, vol. 52, pp. 478-485, 2014.
- [25] S. Thomas, C.H. Chan, L.A. Pothen, J. Joy, and H.J. Maria, *Natural Rubber Materials: Volume 2: Composites and Nanocomposites*, Cambridge, UK: Royal Society of Chemistry, 2013.

- [26] K. Oohira, "Development of an Antenna Materials Based on Rubber that has Flexibility and High Impact Resistance", NTN Technical Review, vol. 76, pp. 58-63, 2008.
- [27] M. Raees, S.H. Dar, and J. Ahmed, "Characterization of Flexible Wearable Antenna based on Rubber Substrate", Int. J. Adv.d Comp. Sci. Appl., vol. 7, pp. 190-195, 2016.
- [28] C.A. Blannis, Antenna Theory: Analysis and Design, 3d ed., Willey, p.770, 2005.
- [29] J. Baker-Jarvis, M.D. Janezic, and D.C. De Groot (2010) "High Frequency Dielectric Measurements", IEEE Instru. Meas. Mag., vol. 13, pp. 24-31, 2010.
- [30] Gupta, S. Sankaralingam, and S. Dhar, (2010) Development of wearable and implantable antennas in the last decade: A review, In: Proc. of Mediterranean Microwave Symposium, Turkey,2010, pp.251-267.
- [31] A. Al-Sehemi, A. Al-Ghamdi, N. Dishovsky, N. Atanasov, and G. Atanasova, "Design and performance analysis of dual-band wearable compact low-profile antenna for body-centric wireless communications".Int. J. Microw. Wirel. T., vol.10, pp. 1175-1185, 2018.